BULLETIN OF THE POLISH ACADEMY OF SCIENCES
TECHNICAL SCIENCES, Vol. 68, No. 3, 2020
DOI: 10.24425/bpasts.2020.133366



# Machining of microholes in Ti-6Al-4V by hybrid micro electrical discharge machining to improve process parameters and flushing properties

T. MUGILAN[1], M.S. AEZHISAI VALLAVI[1], S. SANTHOSH[1], D. SUGUMAR[2], and S. CHRISTOPHER EZHIL SINGH[3]*

[1] Department of Mechanical Engineering, Government College of Technology, Coimbatore, Tamil Nadu, India
[2] Department of ECE, Karunya Institute of Technology and Sciences, Coimbatore, Tamil Nadu, India
[3] Department of Mechanical Engineering, Vimal Jyothi Engineering College, Kannur, Kerala, India



**Abstract.** In this research work, the Ti-6Al-4V material was used for the investigation of machining parameters by means of hybrid micro electrical discharge machining to improve the machining process and reduce the negative effects of debris accumulation in the drilled hole. L9 orthogonal array was used in the Taguchi based grey relational analysis to optimize the parameters such as material removal rate and diametrical accuracy of the machining process for Ti-6Al-4V. This work encompasses the design, development, and calibration of the work piece vibration platform and experimental analysis of the process parameters by means of the hybrid micro electrical discharge machining process. The maximum material removal rate and minimum surface roughness was observed at the current value of 2.5 A, pulse on time is 2 µs and pulse off time is 14.5 µs. The maximum material removal rate was observed for the increase in pulse on time with 14.4 µs and 4 A current level. The diametrical accuracy of the microholes was increased while increasing the pulse off time and decreasing the pulse on time. The fluid flow simulation has been conducted to find out the pressure drop and to know the velocity of the flow inside the hole for the effective flushing of the debris during machining.

**Key words:** hybrid micro electrical discharge machining, Ti-6Al-4V, fluid flow simulation, material removal rate, diametrical accuracy.

## 1. Introduction

Electrical discharge machining is a non-traditional machining process in which material is removed from the work piece by means of electrical current in a dielectric medium. It consists of a work piece and an electrode. Electrical discharge machining is very effective against alloys with high hardness. Electrical discharge machining excels at manufacturing geometrically complex or hard material parts that are extremely difficult to machine by applying conventional machining processes. It is a non-contact machining technique for material removal that works predominantly on materials that are electrically conductive. It is classified as a non-conventional machining process as it does not primarily depend on mechanical forces for material removal. Micro electrical discharge machining process has been growing in significance in recent years for machining particularly difficult materials. These materials find applications in major fields such as the automobile and aerospace industry etc. Thermo-electrical model of the electrical discharge machining process was simulated for computing the flushing properties of dielectric fluids [1]. Effects of different work piece material, electrode material and electrode shape on different process parameters revealed that an electrode made of copper has an optimum tool wear rate [2]. Optimization involved in this present work is Taguchi based work, but this technique wants some pre requisition, such as the design of experiments which are to be conducted [3]. A tangential feed wire electrical discharge grinding method combined with on-line measurement using a charge-coupled device was proposed for improving on-line machining accuracy of micro-electrodes [4]. In many cases, ultrasonic vibrations were induced to measure changes in performance of the electrical discharge machining process while machining the hardest materials [5]. Effects of different dielectric fluids and different electrodes on the micro electrical discharge machining process were observed [6]. The process parameters such as power input and pulse duration are used to predict the temperature distribution, residual stresses and the shape of the crater formed for single pulse discharge. The model has been validated further using experimental data [7]. The influence of process parameters was also presented. Usage of an electrode with a helix angle of 45° and flute depth of 50 $\mu m$ was found to lower machining time down to 37% and by additional 19% for flute depths of 150 $\mu m$. Holes of 661 micrometers in diameter were successfully drilled. It was also found that greater flute depths decrease the machining time [8]. Flushing techniques and feed rates are identified to improve process parameters. Improvement in the flushing rate

*e-mail: edbertefren0420@gmail.com

Manuscript submitted 2019-08-21, revised 2019-12-10, initially accepted for publication 2019-12-20, published in June 2020

of debris using vibration methods results in a decrease in material removal rate and tool wear rate [9, 10]. Connection between electrode material and tool wear rate is explored [11]. Higher aspect ratio can be achieved by effective flushing and cooling of the work piece [12, 13]. Therefore, it is vital to find methods of improving the micro electrical discharge machining process. Hence, in order to improve the electrical discharge machining of Ti-6Al-4V, effective cooling and flushing are important. The major problems which are identified and attempted to be improved in this study are lower material removal rate, higher, poor diametrical accuracy and ineffective flushing.

## 2. Materials and methods

**2.1. Material.** Titanium alloy has been chosen in this research as a work piece for the micro electrical discharge machining process. This is since titanium is difficult to machine, very hard and has a high melting point, making it a suitable candidate to measure the process capability of the micro electrical discharge machining process. The work piece material used in this study is a grade-V titanium alloy (Ti-6Al-4V). The work piece is in the form of a rectangular block of 25×25 mm and thickness of 6 mm. The work piece is then machined to a thickness of 3 mm using a wire electrical discharge machining process. The tool used in this work is a copper electrode of 0.5 mm in diameter.

**2.2. Hybrid micro electrical discharge machining setup.** From the literature survey it was identified that vibration of the work piece was effective in flushing the debris from the spark gap, thereby preventing the formation of secondary sparks and irregular arcing. Machining setup details are shown in Table 1. This can improve the performance of the process by increasing material removal rate and reducing tool wear rate. A custom-built vibration kit is designed for this project. The work piece is to be fixed onto this vibration platform during machining. A schematic diagram of the die sinking electrical discharge machining with the vibration kit is shown in Fig. 1.

Table 1
Machining setup

| Parameters | Specification |
|---|---|
| Work piece | Ti-6Al-4V |
| Work piece dimension | 25×25×3 mm |
| Tool electrode | Copper |
| Coolant | Daphne cut |
| Machine | Mitsubishi EDM EA 8 |

**2.3. Calibration of vibration kit.** In order to identify the amplitude of vibrations and to calibrate the vibration kit, an accelerometer is used. Calibration is vital for the study as it enables us to identify the natural frequency of the work piece and kit setup. This can help us identify the suitable frequencies and amplitudes to induce proper vibrations. Despite the sound generator being able to generate multiple waveforms, namely the sine wave, square wave, saw-tooth wave and triangle wave, the sine wave was fixed as the waveform of choice to ensure that the surface vibrations produced cause minimum damage to the voice coil motor membrane.

A control system is made as shown in Fig. 2 that can interpret the input voltages into acceleration data and, when applying suitable transforms, can be double integrated to yield displacement values. All the data are displayed in graph form by using lab view software. The values of the acceleration and displacement induced by the vibration are provided in both peak value and root mean square value. A spectral graph of the frequency is also displayed.

Before measuring the accelerations of the various frequencies induced, the response of the sensor when no signal is given was first measured and recorded. The goal of this was to identify whether frequency isolation was effective. Any ambient vibrations that could distort the readings would be visible during this trial. From the experiment, it was verified that no induced vibrations were registered. The acceleration and dis-

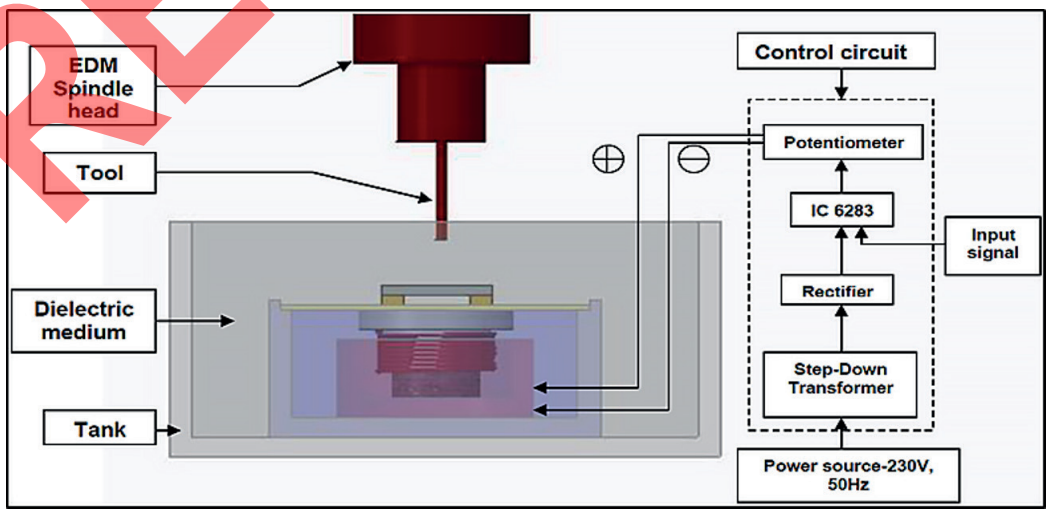


Fig. 1. Schematic diagram of die sinking electrical discharge machining with vibration kit

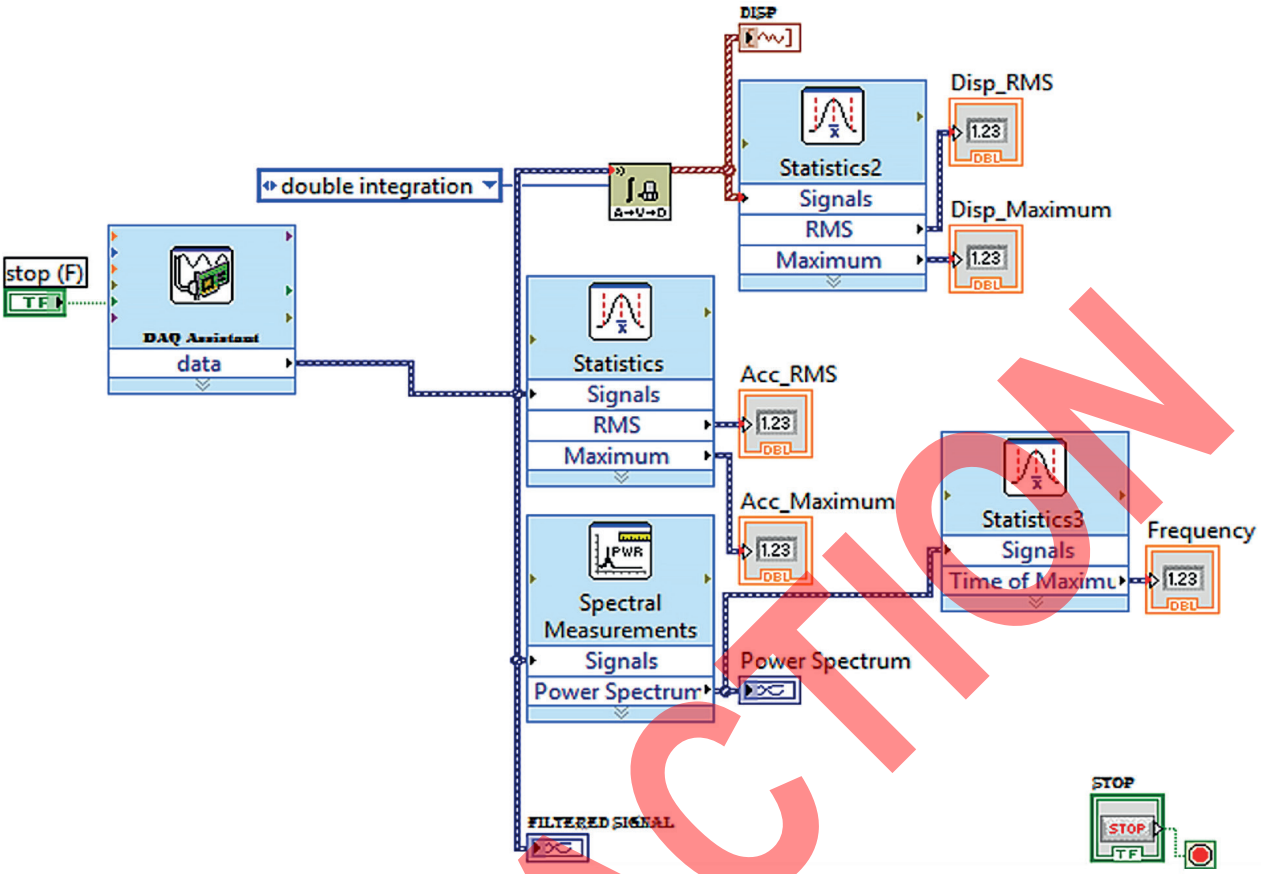


Fig. 2. Control system for measuring values

placement values that are displayed can be linked to unavoidable instrument noise. With the confirmation that the ambient noise has been accounted for and damped, the actual trials for the experiments were conducted. It is observed that despite no observable trends becoming visible in the displacement graph in peak value, a clear peak is visible at 200 Hz of 86.60% of current supply followed by 59.98%, 73.30% and 100% from Fig. 3. This could be considered as the natural frequency of the setup.

Upon examining the acceleration graphs, which should manifest steady upwards trends, it is seen that there is a significant rise at 200 Hz as compared with Fig. 4. This provides confirmation that 200 Hz is the natural frequency of the setup which provides maximum amplitude at all current levels. The experiment requires vibrations to be induced in the range of 30–50 microns in order to ensure that the surface finish of the hole is not sacrificed in pursuit of better flushing. The 30–50 microns amplitude required was found to be produced at 350 Hz at 86.6% current. Hence, this was taken to be the ideal frequency to operate the kit. For additional levels for experimentation, it was noted that maximum amplitude was observed at 200 Hz and medium amplitude at 250 Hz.

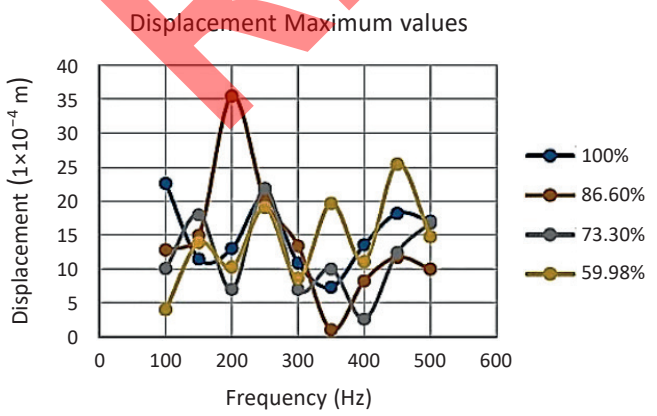


Fig. 3. Maximum displacement values for various frequencies

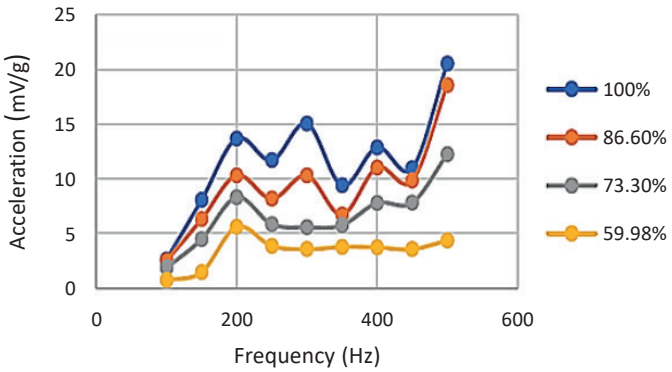


Fig. 4. Maximum acceleration values for various frequencies

**2.4. Experimental design using Taguchi method.** An experiment was conducted with the Ti-6Al-4V alloy work piece and copper electrode in order to study the current operating conditions and performance of the micro electrical discharge machining process. This trial would also facilitate the identification of an optimized set of process parameters for further improvement using the hybrid system. From the literature survey, it was inferred that the process parameters used would be current, pulse on time and pulse off time. These three parameters are to be varied in order to obtain a set of experiments. The technique used for the design of experiments is the Taguchi method with L9 orthogonal array. The three levels and three factors as indicated in A, B and C are used in this work shown in Table 2 and corresponding experimental results are shown in Table 3. The machining is performed on the vibration kit setup with optimized conditions using a different dielectric fluid, and the results are shown in Table 4.

Table 2
Machining parameters and their corresponding levels

| Code | Parameter | Units | Level 1 | Level 2 | Level 3 |
|---|---|---|---|---|---|
| A | Current | *A* | 1 | 2.5 | 4 |
| B | Pulse on | $\mu s$ | 2 | 5.2 | 8 |
| C | Pulse off | $\mu s$ | 2 | 6.4 | 14.4 |

Table 3
Machining time, material removal rate (MRR) and diametrical accuracy (DA)

| Trial No. | Current (A) | Pulse on ($\mu s$) | Pulse off ($\mu s$) | Machining time (min) | MRR ($10^{-3}$ mm$^3$/min) | DA (mm) |
|---|---|---|---|---|---|---|
| 1 | 1 | 5.2 | 2 | 122 | 7.044 | 0.168 |
| 2 | 1 | 2 | 6.4 | 103 | 7.926 | 0.466 |
| 3 | 1 | 8 | 14.4 | 101 | 11.011 | 0.143 |
| 4 | 4 | 5.2 | 6.4 | 96 | 7.097 | 0.326 |
| 5 | 4 | 2 | 14.4 | 29 | 43.118 | 0.222 |
| 6 | 4 | 8 | 2 | 83 | 17.349 | 0.19 |
| 7 | 2.5 | 5.2 | 14.4 | 42 | 27.315 | 0.347 |
| 8 | 2.5 | 2 | 2 | 86 | 12.631 | 0.282 |
| 9 | 2.5 | 8 | 6.4 | 46 | 16.221 | 0.243 |

Table 4
Machining parameters with vibration kit

| Current (*A*) | Pulse on ($\mu s$) | Pulse off ($\mu s$) | Machining time (min) | MRR ($10^{-3}$ mm$^3$/min) | Dielectric | Frequency (Hz) | Input signal (%) |
|---|---|---|---|---|---|---|---|
| 2.5 | 2 | 14.4 | 75 | 10.29 | Daphne cut | Nil | Nil |
| 2.5 | 2 | 14.4 | 63 | 14.07 | | 250 | 73.3 |
| 2.5 | 2 | 14.4 | 49 | 14.82 | | 350 | 86.67 |
| 2.5 | 2 | 14.4 | 88 | 12.56 | | 200 | 100 |
| 2.5 | 2 | 14.4 | 57 | 15.98 | Graphene + Aluminum + Daphne cut | Nil | Nil |
| 2.5 | 2 | 14.4 | 46 | 23.26 | | 350 | 86.67 |

**2.5. Hybrid micro electrical discharge machining process.** The vibration platform was successfully assembled and calibrated. Experimentation with various frequencies of vibration and dielectric combinations could be carried out on the Ti-6Al-4V work piece. From the calibration phase, three frequencies and amplitudes of vibration were chosen. These three levels, which operate at the previously optimized machining parameters, form the basis of the experimentation of the vibration set-up. The material removal rate of these three levels is compared with each other to identify optimum frequency of operation. This is then used as the operating parameters for the dielectric medium with additives. The machining parameters are tabulated in Table 5.

Table 5
Machining parameters for hybrid setup

| Current (*A*) | Pulse on ($\mu s$) | Pulse off ($\mu s$) | Machining time (min) | MRR ($10^{-3}$ mm$^3$/min) | Dielectric | Frequency (Hz) | Input signal (%) |
|---|---|---|---|---|---|---|---|
| 2.5 | 2 | 14.4 | 75 | 10.29 | Daphne cut | Nil | Nil |
| 2.5 | 2 | 14.4 | 63 | 14.07 | Daphne cut | 250 | 73.3 |
| 2.5 | 2 | 14.4 | 49 | 14.82 | Daphne cut | 350 | 86.67 |
| 2.5 | 2 | 14.4 | 88 | 12.56 | Daphne cut | 200 | 100 |
| 2.5 | 2 | 14.4 | 57 | 15.98 | Graphene + Aluminum + Daphne cut | Nil | Nil |
| 2.5 | 2 | 14.4 | 46 | 23.26 | | 350 | 86.67 |

The experiments of machining the work piece with the hybrid kit incorporated were conducted and their results were tabulated in Table 4. Upon studying the results, it can be observed that the maximum material removal rate was observed for the trial performed at 350 Hz and with the dielectric (Graphite + Aluminum + Daphne cut) setup.

An inference can be made that the vibrations imparted to the work piece facilitated the flushing of debris from the spark gap and prevented secondary sparks. This led to the increase in material removal rate on Ti-6Al-4V as the probability of secondary sparking was significantly reduced due to the lack of residual debris. Thus, the process reached an optimum material removal rate and the performance of the process has seen a significant increase. The experiment was also focused on reducing the tool wear rate. However, upon conducting both the preliminary and final experiments, an observation was made regarding the weight of the tool electrodes. It was observed that the tool electrode's weight almost always marginally increased after machining. This meant that the actual tool wear rate could not be accurately calculated. Upon investigation, black deposition was observed on the tip of all the electrodes after the machining had occurred, as shown in Fig. 5.

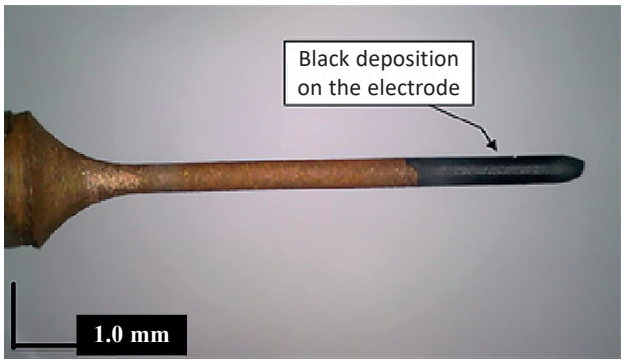


Fig. 5. Black tip of the electrode

**2.6. Taguchi based grey relational analysis.** Grey relational analysis is used for solving inter-relationships among multiple responses. In this approach, a grey relational grade is obtained for analyzing the relational degree of multiple responses. Table 6 shows the S/N ratios and normalization values for material removal rate and diametrical accuracy. Table 7 depicts the grey relational coefficients and grey relational grade for the material removal rate and the diametrical accuracy in optimization.

Table 6
S/N Ratios and normalized S/N ratios of material removal rate (MRR) and diametrical accuracy (DA)

| Trail No. | S/N ratio | | Normalized S/N ratios | |
|---|---|---|---|---|
| | MRR | DA | MRR | DA |
| 1 | –43.04 | 15.49 | 0.000 | 0.14 |
| 2 | –42.02 | 06.63 | 0.065 | 1.00 |
| 3 | –39.16 | 16.89 | 0.247 | 0.00 |
| 4 | –42.98 | 09.74 | 0.004 | 0.70 |
| 5 | –27.31 | 13.07 | 1.000 | 0.37 |
| 6 | –35.21 | 14.42 | 0.498 | 0.24 |
| 7 | –31.27 | 09.19 | 0.748 | 0.75 |
| 8 | –37.97 | 10.99 | 0.322 | 0.57 |
| 9 | –35.80 | 12.29 | 0.460 | 0.45 |

Table 7
Grey relational coefficients (GRC) and grey relational grade (GRG) for material removal rate and diametrical accuracy (DA)

| Trail No. | Normalized S/N | | Deviation | | GRC | | GRG |
|---|---|---|---|---|---|---|---|
| | MRR | DA | MRR | DA | MRR | DA | |
| 1 | 0.000 | 0.14 | 1.00 | 0.56 | 0.50 | 0.31 | 0.41 |
| 2 | 0.065 | 1.00 | 0.94 | –0.30 | 0.52 | 1.00 | 0.76 |
| 3 | 0.247 | 0.00 | 0.75 | 0.70 | 0.57 | 0.28 | 0.43 |
| 4 | 0.004 | 0.70 | 0.99 | 0.00 | 0.50 | 0.57 | 0.53 |
| 5 | 1.000 | 0.37 | 0.00 | 0.33 | 1.00 | 0.39 | 0.69 |
| 6 | 0.498 | 0.24 | 0.50 | 0.46 | 0.67 | 0.34 | 0.50 |
| 7 | 0.748 | 0.75 | 0.25 | –0.05 | 0.80 | 0.61 | 0.71 |
| 8 | 0.322 | 0.57 | 0.68 | 0.12 | 0.60 | 0.48 | 0.54 |
| 9 | 0.460 | 0.45 | 0.54 | 0.25 | 0.65 | 0.42 | 0.53 |

## 3. Results and discussion

**3.1. Effect of fluid flow flushing on machining of Ti-6Al-4V.** In order to find out the pressure drop and to know the velocity of the flow inside the hole for the effective flushing of the debris formed during machining, simulation of the same is carried out in ANSYS Fluent software. The convergent nozzle is acting as control volume, which is shown in Fig. 6. From Fig. 7, it is seen that velocity inside the hole is higher in the case of a nozzle located away from the hole. The velocity (as shown in Fig. 7) inside the hole is nearly 4 m/s.

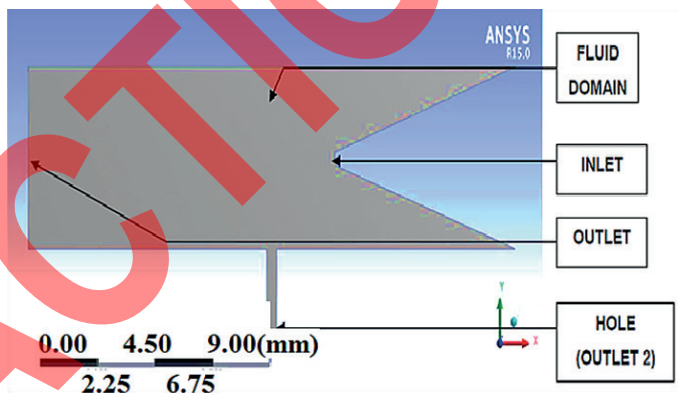


Fig. 6. Convergent nozzle

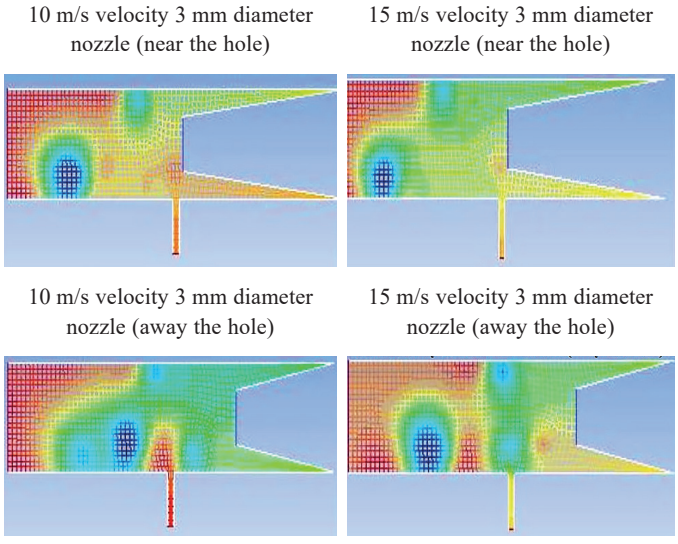


Fig. 7. Pressure variations at various velocities

It can be concluded that better results could be obtained if the location of the nozzle is away from the hole so that the pressure drop zone is located near the hole.

The simulation is continued until the solution converges. Pressure drops for the different conditions as stated above are found initially. The pressure drops for 10 m/s velocity and 3 mm diameter nozzle (near the hole), 15 m/s velocity and 3 mm diameter nozzle (near the hole), 10 m/s velocity and 3 mm diameter nozzle (away from hole) as well as the pressure drop for 15 m/s velocity and 3 mm diameter nozzle (away from hole) are all shown in Fig. 7. From the results, it was seen that pressure drop exists when the fluid flows near the hole. This change in pressure would be essential for carrying the solid debris particles formed during the machining process. As the distance of the nozzle increases from the hole, we can see that the pressure zone also changes. Thus, the location of the convergent nozzle is also significant.

**3.2. Effect of pulse on time on material removal rate.** The effect of pulse on time and current on material removal rate is shown in Fig. 8. It clarifies the relationship between the pulse on time and material removal rate with changes in current levels. The variation in pulse on time with a constant current level shows the variation in material removal rate which is the increasing pulse on time at 1 *A* combined with increasing the material removal rate. Decreasing material removal rate is observed from the moment of increasing the pulse on time at current level of 2.5 *A*. The highest material removal rate was observed at pulse on time of 2 *μs* with current level of 4 *A*.

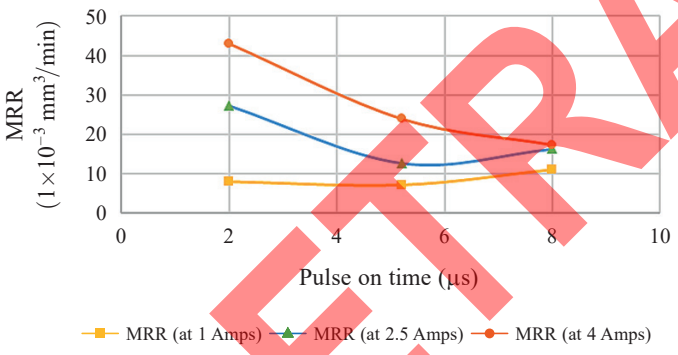


Fig. 8. Pulse on time vs material removal rate

**3.3. Effect of pulse off time on material removal rate.** Figure 9 shows the relation between the pulse off time and material removal rate with respect to current in *A*. For a constant 1 *A* current level with variation of pulse off time the material removal rate is increasing gradually with increase of the pulse off time. Like in the case of the 2.5 *A* current level, with variation in pulse off time the material removal rate is increased for the Ti-6Al-4V alloy.

The maximum increase of pulse off time is reached gradually. Like in the case if the 2.5 *A* current level, with variation in pulse off time the material removal rate is increased for the Ti-6Al-4V alloy. The maximum amount of material removal rate was observed from the 14.4 *μs* pulse off time for all levels of current in *A*. As compared to the other values of material

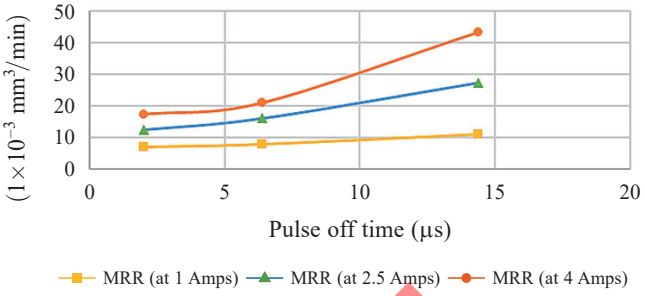


Fig. 9. Pulse off time vs material removal rate

removal rate, the maximum value was achieved at the 4 *A* current with 14.4 *μs* pulse off time.

**3.4. Effect of pulse on time on diametrical accuracy.** Figure 10 presents the effect of pulse on time on diametrical accuracy with respect to input current. Increasing the pulse on time gives the results of decreasing diametrical accuracy at 1 *A* input current, with minimum diametrical accuracy achieved at 2 *μs* input pulse on time. Maximum diametrical accuracy was observed for both cases as 2.5 *A* with 2 *μs* pulse on time while machining the Ti-6Al-4V alloy. Minimum diametrical accuracy was observed with the increase of pulse on time. The higher time duration of pulse on time leads to less diametrical accuracy.

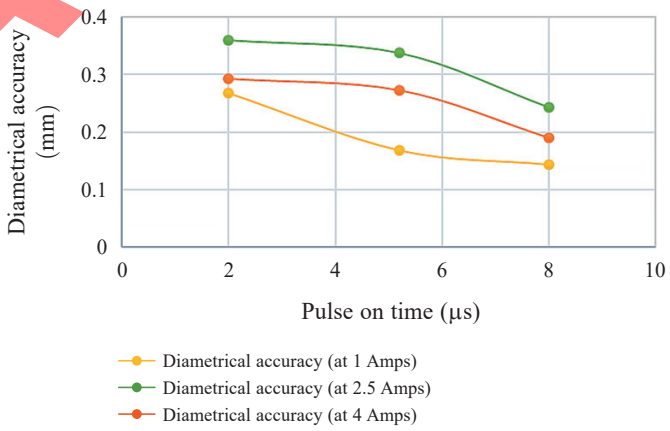


Fig. 10. Pulse on time vs diametrical accuracy

**3.5. Effect of pulse off time on diametrical accuracy.** The effect of pulse off time on diametrical accuracy with input current is shown in Fig. 11. The highest accuracy of the micro-hole diameter in the Ti-6Al-4V alloy was observed for the highest pulse off time values.

The 4 *A* input current with 14.4 *μs* input pulse off time gives the higher diametrical accuracy, followed by 2.5 *A* input current with 14.4 *μs* input pulse off time and 1 *A* current and 14.4 *μs* pulse off time giving less accuracy as compare to all experimental results values. Increasing pulse off time gives good diametrical accuracy.

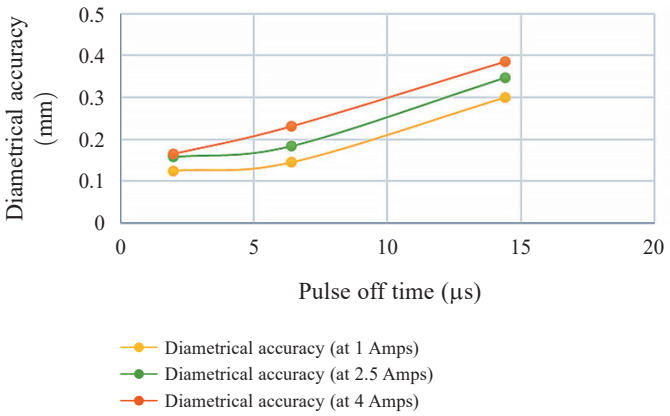


Fig. 11. Pulse off time vs diametrical accuracy

**3.6. Analysis of variance for grey relational grade.** The results of ANOVA for grey relational grade are shown in Table 8. The factors of current, pulse on time and pulse off time are significant as their P- value is less than 0.05, which was inferred from the ANOVA Table. So that the most influential micro electrical discharge machining parameter is pulse off time, which contributes in 38.37% towards the machinability of producing micro holes for a given material removal rate and surface roughness of the Ti-6Al-4V alloy. That means the pulse off time controls the performance of the machining process and it leads to effective machining of Ti-6Al-4V towards the expected output responses. The adequacy of this analysis is set at a 95% level of confidence for the micro electrical discharge machining process parameters and the output machining responses. The achieved R-sq value is 97.25%. The next significant parameter followed by pulse off time is pulse on time, which contributes 31.30%, and then current, with a 25.31% contribution towards the machinability of producing the micro holes on the titanium alloy.

Table 8
ANOVA for grey relational grade

| Source | DF | Adj SS | Adj MS | F-value | P-value | Cont. % |
|---|---|---|---|---|---|---|
| Current | 2 | 0.031 | 0.016 | 0.81 | 0.045 | 25.31 |
| Pulse on time | 2 | 0.039 | 0.019 | 0.96 | 0.046 | 31.30 |
| Pulse off time | 2 | 0.048 | 0.024 | 1.23 | 0.035 | 38.37 |
| Error | 2 | 0.006 | 0.003 | – | – | 5.02 |
| Total | 8 | 0.124 | – | – | – | 100 |

**3.7. Optimization of machining parameters.** The changes of the machining parameter conditions from one trail to another leads to more effective analysis and understanding of the behavior of the machining parameter towards the output response, i.e. material removal rate and Ra. Table 9 shows the response for the grey relation grade at each level, which is very useful for interpreting the relation between the parameter setting for optimum levels and producing the micro holes in a hybrid setup.

Table 9
Grey relational grade for each level

| Factors | Current | Pulse on time | Pulse off time |
|---|---|---|---|
| Level 1 | 0.531 | **0.664** | 0.483 |
| Level 2 | **0.593** | 0.549 | 0.609 |
| Level 3 | 0.577 | 0.488 | **0.609** |
| Delta | 0.062 | 0.175 | 0.125 |
| Rank | 3 | 1 | 2 |

Figure 12 presents the effects of the machining parameters and optimum condition setting. A large deviation is observed from pulse off time, so it contributes most towards machining performance improvement, and is followed by pulse on time and current.

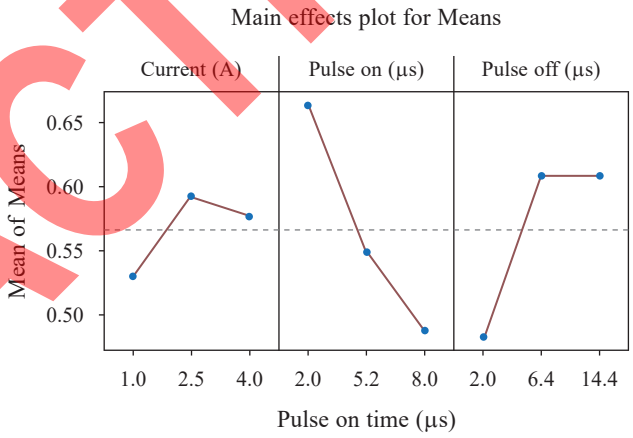


Fig. 12. Setting of optimized parameters

The setting of optimum machining condition leads to minimum surface roughness and maximum material removal rate. Table 10 presents the optimized values for each input machining parameter. The optimized current value is 2 *A*, pulse on time is 2 $\mu s$ and pulse off time is 14.4 $\mu s$.

Table 10
Optimized parameters

| Parameters | Values |
|---|---|
| Current (*A*) | 2.5 |
| Pulse on time ($\mu s$) | 2 |
| Pulse off time ($\mu s$) | 14.4 |

**3.8. Micro hole images and material removal rate.** The maximum material removal rate is observed under optimum machining conditions. The micro hole images produced under such

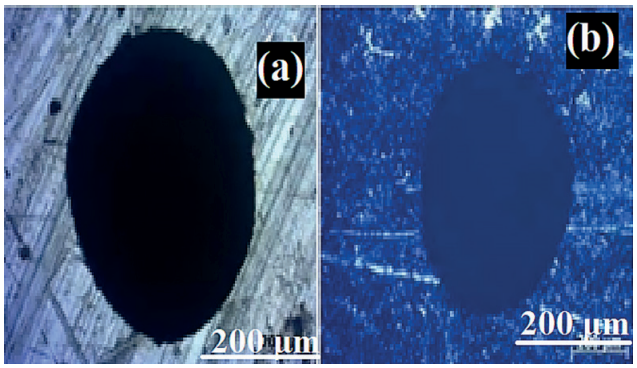


Fig. 13. (a) Front surface and (b) back surface image of the machined sample at peak current of 2 *A*, pulse ON Time of 2 $\mu s$ and pulse OFF time of 14.4 $\mu s$

conditions are shown in Fig. 13a and 13b. It was observed that the tool electrode's weight almost always marginally increased after machining. This meant that the actual material removal rate could not be accurately calculated. Upon investigation, black deposition was observed on the tip of all the electrodes after the machining had occurred.

**3.9. Effect of titanium deposition on electrode.** From the EDAX spectrum it can clearly be seen that there is a significant (6.28% by weight) presence of titanium on the electrode, as shown in Fig. 14. This means that the black deposit on the copper electrode is the mixture of elements as tabulated in Table 11. This explains the reason for the increase in tool weight. Thus, we can infer that, despite tool wear occurring, the deposition of titanium on the surface of the electrode is able to compensate for that material removal rate.

Table 11
Weight % of elements in the black deposition

| Element | C | O | Cu | Zn | Al | Ti |
|---|---|---|---|---|---|---|
| Weight % | 41.73 | 4.33 | 46.58 | 0.72 | 0.36 | 6.28 |

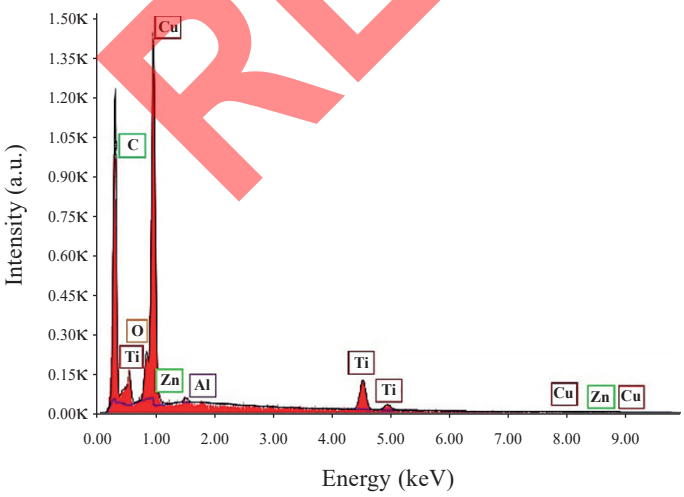


Fig. 14. EDAX test result for the black deposition on tip of the electrode

**3.10. Effect of surface roughness.** The surface roughnesses of the holes on the Ti-6Al-4V work-piece being cut were evaluated by exposing the inner surface of the hole and using a surface roughness tester to measure the profile of the holes. The results of the test are shown in Table 12.

Table 12
Surface roughness test

| Part No. | Description | Surface roughness ($\mu m$) |
|---|---|---|
| 1 | Without vibration, Dc | 3.188 |
| 2 | With vibration at 350 Hz, Dc | 1.741 |
| 3 | Without vibration, Gr + Al + Dc | 1.867 |
| 4 | With vibration at 350 Hz, Gr + Al + Dc | 2.030 |

From the above Table 12, we infer that the use of vibrations during machining has led to the improvement of surface finish. There is a significant decrease in surface roughness with the implementation of the hybrid electrical discharge machining kit. An inference can be made that surface roughness can be reduced with the implementation of a vibration platform, as the vibration removes debris that causes unstable secondary sparking; additives to the dielectric medium serve mainly to increase the material removal rate and do not significantly affect surface roughness.

## 4. Conclusion

In conclusion, the micro electrical discharge machining process was studied and its process parameters were understood in order to find ways to improve the performance of the machine. As per the objectives of the study:

Machining of micro-holes was carried out on Ti-6Al-4V by means of micro electrical discharge machining.

The process parameters such as pulse on time, pulse off time and current and their effects on performance characteristics such as the material removal rate were studied and an optimized set of parameters was obtained. Optimized current value is 2 *A*, pulse on time is 2$\mu s$ and pulse off time is 14.4$\mu s$.

A hybrid micro electrical discharge machining kit was designed and implemented and was observed to successfully improve material removal rate of the machining process on Ti-6Al-4V with increasing the pulse off time.

A computational fluid dynamics model was generated and studied to get a better understanding of flushing properties.

Methods for proper integration of vibration into the micro electrical discharge machining machine and the reasons for the deposition of titanium were also discussed.

The hybrid micro electrical discharge machining kit development was able to increase the material removal rate by allowing for better flushing capabilities. It was observed that black deposits on the tool were titanium deposits and they caused the electrode to increase in weight.

## Reference

[1] E. Weingärtner, F. Kuster, and K. Wegener, "Modeling and simulation of electrical discharge machining", *Procedia CIRP* 2, 74–78 (2012).

[2] G. D'Urso and C. Merla, "Workpiece and electrode influence on micro–EDM drilling performance", *Precis. Eng.* 38(4), 903–914 (2014).

[3] K. Krishnaiah and P. Shahabudeen, "Applied design of experiments and Taguchi methods", PHI Learning Pvt. Ltd., 2012.

[4] L. Zhang, T. Hao, and Y. Li, "Precision machining of micro tool electrodes in micro EDM for drilling array micro holes" *Precis. Eng*. 39, 100–106 (2015).

[5] M.M. Sundaram, G.B. Pavalarajan, and K.P. Rajurkar, "A study on process parameters of ultrasonic assisted micro EDM based on Taguchi method", *J. Mater. Process. Technol*. 17(2), 210–215 (2008).

[6] D. Tanikić, V. Marinković, M. Manić, G. Devedžić, and S. Ranđelović, "Application of response surface methodology and fuzzy logic based system for determining metal cutting temperature", *Bull. Pol. Ac.: Tech*. 64(2), 435–445 (2016).

[7] Das Shuvra, M. Klotz, and F. Klocke, "EDM simulation: finite element–based calculation of deformation, microstructure and residual stresses", *J. Mater. Process. Technol*. 142(2), 434–451 (2003).

[8] S. Plaza, J.A. Sanchez, E. Perez, R. Gil, B. Izquierdo, N. Ortega, and I. Pombo, "Experimental study on micro EDM–drilling of Ti6Al4V using helical electrode", *Precis. Eng.* 38(4), 821–827 (2014).

[9] Y.S Liao and H.W. Liang, "Study of vibration assisted inclined feed micro–EDM drilling", *Procedia CIRP* 42, 552–556 (2016).

[10] Y. Jiang, W. Zhao, X. Xi, X. Kang, and L. Gu, "Vibration assisted EDM of small–hole using voice coil motor", *Procedia CIRP* 1, 645–650 (2012).

[11] Y. Fu, T. Miyamoto, W. Natsu, W. Zhao, and Z. Yu, "Study on influence of electrode material on hole drilling in micro-EDM." *Procedia CIRP* 42, 516–520 (2016)

[12] D. Rajeev, D. Dinakaran, and S.C.E. Singh, "Artificial neural network based tool wear estimation on dry hard turning processes of AISI4140 steel using coated carbide tool", *Bull. Pol. Ac.: Tech*. 65(4), 553–559 (2017).

[13] F. Eleonora, V. Castiglioni, F. Ceyssens, M. Annoni, D. Reynaerts, and B. Lauwers, "EDM drilling of ultra-high aspect ratio micro holes with insulated tools", *CIRP Annals* 62(10), 191–194, (2013).